AN AUTOMATIC MOSAICKING METHOD FOR BUILDING FACADE TEXTURE MAPPING

Zhizhong Kang[a, *], Liqiang Zhang[b], Sisi Zlatanova[c]

[a]Faculty of Aerospace Engineering, Delft University of Technology, 2629 HS Delft, The Netherlands - Z.Kang@tudelft.nl

[b]Research Center for Remote Sensing and GIS, School of Geography, Beijing Normal University, Beijing, China - zhanglq@bnu.edu.cn

[c]OTB Research Institute for Housing, Urban and Mobility Studies, Delft University of Technology, 2628 BX Delft, The Netherlands - S.Zlatanova@otb.tudelft.nl

KEY WORDS: Terrestrial imaging, Digital camera, Strip model, Mosaicking, Building facade, Texture mapping, Image rectification, Least-square adjustment

ABSTRACT:

This paper presents an automatic mosaicking method for generating building facade texture from a sequence of color close-range digital camera images. The constraint of straight line bundle and the constraint of known orientation of parallel lines in object space are used for determining the digital camera's parameters. Similar to the strip block adjustment used in aerial triangulation, a strip model of the least-square adjustment is used to determine the relative spatial relationship of the image sequence. Then a method similar to orthophoto generation is employed to generate the entire building facade texture. Our results demonstrated that this method is proved to be more applicable. Two refining strategies are presented to optimize the mosaic result. One is refining the mosaic region where corresponding points are difficult to be matched but there are plenty of horizontal lines. The constraint of correspondingly horizontal lines is introduced to implement this process. The other is refining the mosaic region by densifying the corresponding points according to the relatively spatial relationship of the image sequence.

1. INTRODUCTION

Three-dimensional (3D) spatial models of urban environments are useful in variety of today's applications ranging from urban planning, virtual tourism, heritage protection, to training and simulation for urban disaster and emergency scenarios. Digital images acquired by remote sensing techniques from terrestrial, airborne, spaceborne platforms are currently one of the most important data sources to create and update such models. Airborne and satellite imagery has been used for the extraction of texture information of the top surface of the 3D cartographic objects (e.g., terrain and buildings). [1] For the production of fly-through or walk-through and 3D views to assist environmental planning and disaster management, detailed texture information on building facades is also required and can be acquired by terrestrial imaging techniques. Since the lack of the index of image sequences, the processes of image searching, preprocessing, and corresponding are still implemented manually. As a result, the extraction of building facade texture is a time-consuming and labor-intensive task. An alternative, fast and low-cost option is urgently needed.

Frueh et al. 2004 presented an approach to texture mapping a 3D city model obtained from aerial and ground-based laser scans with oblique aerial imagery. In their method, the images are first automatically registered by matching 2D image lines with projections of 3D lines from the city model. Then, for each triangle in the model, the optimal image is selected by taking into account occlusion, image resolution, surface normal orientation, and coherence with neighboring triangles. Finally, the utilized texture patches from all images are combined into one texture atlas for compact representation and efficient rendering. In (Antone et al. 2000) 3D models are created using

*Corresponding author. Tel: +31-15-278-8338; fax: +31-15-278-2348.

lines extracted from merged camera images. (Stamos et al. 2000, Thrun et al. 2000) use laser scanners mounted on a mobile robot for scanning buildings, but the time required for data acquisition of a entire city is prohibitively large; also, the reliability of autonomous mobile systems in outdoor environments is still relatively poor. In (Früh, C. et al. 2001) a method that is capable of rapidly acquiring 3D model and texture data of an entire city at the ground level by using fast 2D laser scanners and digital cameras. This approach has the advantage that data can be acquired continuously, rather than in a stop-and-go fashion, and is therefore much faster than existing methods. The data acquisition system is mounted on a truck moving at a normal speed on public roads, collecting data to be processed offline. Relative position changes can be computed with centimeter accuracy by matching successive laser scans against each other; however, small errors and occasional mismatches can accumulate to a significantly large level in global position estimation of the acquisition vehicle, and hence the 3D reconstructed models, after only a few hundred meters. In (Takase et al. 2003) a system for automatic generation of 3D city models has been developed, using laser profiler data, 2D digital map, and aerial image, which are processed by the software newly developed. MapCube, the 3D city models generated by the system, has already covered all major cities of Japan at the end of 2002. Applications for virtual reality (VR) that deal with accurate and photo-realistic 3D city models are becoming indispensable in many fields.

The acquisition of building facades textures from vehicle-based digital imaging sensors has advantages in resolution and convenience over oblique airborne images and rapidness. This essential advantage makes land-based mobile mapping systems very useful in collecting 3D city models and other photorealistic walkthrough or drive-through applications. Usually for large and tall buildings, several images, instead of only one image, are required to cover the facade texture of the whole building. A mosaicking process therefore is required in order to obtain the whole facade texture. At present, existing commercial image mosaicking software packages are mainly developed to process either satellite and aerial images such as ERSI's eYaMosaic and Supresoft's ImageXuite, or digital camera images to create the virtual reality panoramic images such as Panaroma Factory, MGI PhotoVista, and Cannon PhotoStitch. All of them show satisfactory performance when processing images with small geometric distortion. However, images acquired by land-based mobile mapping sensors have large obliquity due to the attitude and direction of the digital imaging sensors which leads to considerable geometric distortion. Therefore, alternative image mosaicking methods that could handle such geometric distortion are needed.

Because building facades are usually planar, there are two groups of lines parallel to *X*-axis and *Y*-axis in object space which are possible to be automatically extracted from imagery. Therefore the automatic rectification and mosaicking of such images are feasible. This study attempts to develop a novel automatic mosaicking algorithm for building facade texture mapping using a monocular close-range digital image sequence. The process follows four steps, i.e. image rectification, subsection of image sequence, image mosaic and refining of mosaic result. In the sections that follow, our approach for automatic mosaicking of such an image sequence with considerable geometric distortion will be described, tested, and discussed.

2 IMAGE RECTIFICATION

Since the oblique angle of close-ranged DC images is large, facade texture in the image has obvious geometric distortion. Therefore, the process of rectification of raw image is necessary to acquire the texture similar to real facade.

The key of image rectification is how to compute orientation parameters (except the coordinates of projective center) using image information. The algorithm presented in this paper is based on vanishing point geometry and the geometric constrains of known orientation of parallel object lines.

Since building facades are planar, there are two groups of lines parallel to *X*-axis and *Y*-axis in object space respectively on each of them. As a result, only focus f and three angular orientation parameters φ, ω, k can be calculated according to theories of vanishing point geometry. Facade textures are accordingly rectified using f, φ, ω, k and the principle point which is fixed at the center of image in this case. The process of rectification is illustrated as Fig.1. P is the original image and P_0 is the rectified image of P on the plumb plane.

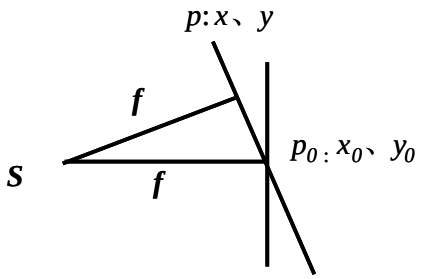

Fig.1 The process of rectification

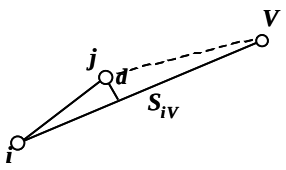

Fig.2 The constrain of Straight lines bundle

Straight lines are extracted in the image. Lines parallel to *X*-axis and *Y*-axis in object space respectively are use to calculate the vanishing points. Vanishing point $V(x_V, y_V)$ is the intersection point of a set of straight lines which are parallel with each other in object space. Accordingly, each straight line, e.g. line *ij*, belonging to this set should pass through the vanishing point as shown in Fig.2. Therefore Eqs.1 is evolved.

$$d = (y_j - y_i)\frac{(x_V - x_i)}{s_{iV}} - (x_j - x_i)\frac{(y_V - y_i)}{s_{iV}} \qquad (1)$$

Where, *d* is the distance of point *j* to line *iV*;

S_{iv} is the distance between point *i* and vanishing point *v*.

Then initial values of DC angular parameters are decomposed according to vanishing point geometry (Caprile, B. et al. 1990). According to the vanishing point geometry the relationship of vanishing point and DC orientation parameters is deduced as Eqs.2.

$$\left.\begin{aligned} x_{X\infty} &= x_0 + f\cot\varphi\sec\omega\cos\kappa - f\tan\omega\sin\kappa \\ y_{X\infty} &= y_0 - f\cot\varphi\sec\omega\sin\kappa - f\tan\omega\cos\kappa \\ x_{Y\infty} &= x_0 + f\sec\omega\csc\omega\sin\kappa - f\tan\omega\sin\kappa \\ y_{Y\infty} &= y_0 + f\sec\omega\csc\omega\cos\kappa - f\tan\omega\cos\kappa \\ x_{Z\infty} &= x_0 - f\tan\varphi\sec\omega\cos\kappa - f\tan\omega\sin\kappa \\ y_{Z\infty} &= y_0 + f\tan\varphi\sec\omega\sin\kappa - f\tan\omega\cos\kappa \end{aligned}\right\} \qquad (2)$$

Thereafter, vanishing point coordinate (x_V, y_V) in Eqs.1 is replaced with interior and exterior orientation (angular) parameters according to Eqs.2. A model of adjustment system of observations and parameters employed the constraint of straight lines bundle is then deduced to calibrate DC angular parameters. The interior orientation parameters are fixed in the adjustment system. Because the initial value of orientation parameters is decomposed from vanishing point coordinates, the accuracy is not always high owing to the quality of images and the error of line extraction. Therefore, it has a small convergent radius that the model of adjustment system employed the constraint of straight lines bundle. The model of adjustment system is not robust accordingly.

In this article, the constraint of known orientation of parallel lines in object space is introduced to control the adjustment system.

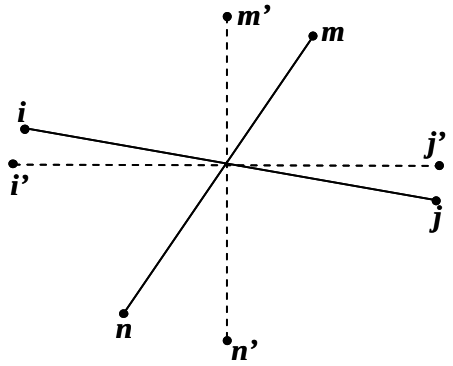

Fig.3 the constraint of known orientation of parallel lines in object space

There are two group lines parallel to *X*-axis and *Y*-axis in object space respectively. The projections of these two group lines in rectified image P_0 should be parallel to *X*-axis and *Y*-axis in object space respectively in ideal instance. Namely Eqs.3 and 4 are deduced.

In *X* direction:

$$-f\frac{b_1x_i + b_2y_i - b_3f}{c_1x_i + c_2y_i - c_3f} = -f\frac{b_1x_j + b_2y_j - b_3f}{c_1x_j + c_2y_j - c_3f} \qquad (3)$$

In *Y* direction:

$$-f\frac{a_1x_m + a_2y_m - a_3f}{c_1x_m + c_2y_m - c_3f} = -f\frac{a_1x_n + a_2y_n - a_3f}{c_1x_n + c_2y_n - c_3f} \qquad (4)$$

Where:

$(x_i, y_i), (x_j, y_j)$: the coordinates of two end points of line parallel to X-axis

$(x_m, y_m), (x_n, y_n)$: the coordinates of two end points of line parallel to Y-axis

f: focal length

$\begin{bmatrix} a_1 & a_2 & a_3 \\ b_1 & b_2 & b_3 \\ c_1 & c_2 & c_3 \end{bmatrix}$: rotation matrix

Eqs.3 and 4 can be control condition for the calibration of DC angular parameters. Therefore it's deduced that a model of adjustment system combined with constraints of straight lines bundle and known orientation of parallel lines in object space. The rigidly geometric constraint is imposed on the adjustment system, therefore the model of adjustment system deduced here has the characteristics of large convergent radius and high stability.

3. IMAGE SEQUENCE SUBSECTION

To recover building facade texture from image sequence efficiently, the image sequence should be automatically subsected into segments corresponding to each building. Accordingly, the histogram of projective difference of corresponding points is used for automatic image sequence subsection.

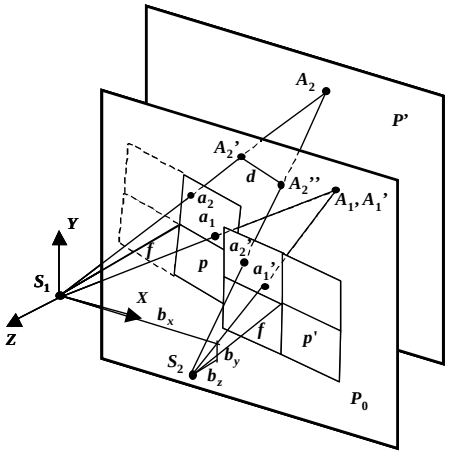

Fig.4 The projective geometry of corresponding points

As Fig.4, the origin of the coordinate system chosen in this paper is the projective center S_1 of the first image. The plane XY is parallel to the facade. The ideal image plane P_0 of the first image (the distance between point S_1 and P_0 is focus f) is considered as public projective plane. As far as corresponding point on the facade a_1 and a_1' be concerned, the projective difference between their projection point A_1 and A_1' should be very small or even ideal zero. However, projection point A_2 and A_2' of corresponding point a_2 and a_2' not on the facade have large projective difference (Fig.4). Accordingly 1-D histogram along x-axis of image coordinate system is drawn to show the distribution of projective difference (Fig.5).

Cross-road and facades having large range variance with each other (Fig.6) are represented in the histogram by peak areas. Moreover, the location of range variance in image is indicated by the location of corresponding peak area in the histogram because the histogram is drawn following the moving direction of vehicle. According to the location indicated, images including cross-road are excluded from image sequence and image segment corresponding to each building is extracted from image sequence.

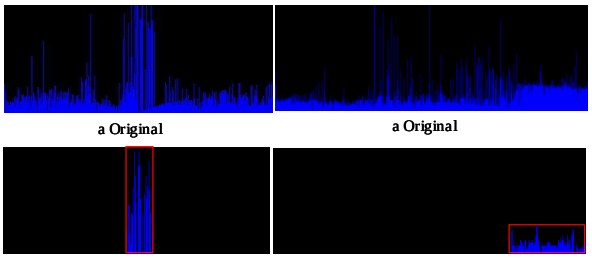

Fig.5 the histogram of projective difference of corresponding points

a. Cross-road b. Connected buildings with large range variance

Fig.6 Segments with large range variance

4. THE AUTOMATIC MOSAIC OF FACADE TEXTURE

Usually for big buildings, facade texture is covered by several images instead of only one image. Therefore to acquire the whole facade texture, mosaic process is required. In this paper, a strip method for image mosaic is presented. A model of least square adjustment is deduced to determine the relatively spatial relationship of the image sequence. This model is similar to the one of the strip block adjustment using in aerial triangulation and based on the formula of the projection of image point on the projective plane. In this model the DC angular parameters

determined after the process of rectification are considered as weighted observation.

In this paper, the facade is considered as a plane and parallel to the public projective plane P_0 (Fig.4). Therefore, the relatively spatial relationship of the image sequence will be recovered when the corresponding rays of each two images intersect on the public projective plane via adjusting the exterior orientation parameters (EOPs) of each image. According to the relatively spatial relationship of the image sequence determined above, a method similar ortho-image generation is employed to recover the whole facade texture.

Firstly, the formula, describing the projective relationship as Fig.4, is deduced as below based on the projective formula of image point on the projective plane.

$$\left.\begin{aligned} &-(f+Z_{S1})\frac{a_{11}x_1+a_{12}y_1-a_{13}f}{c_{11}x_1+c_{12}y_1-c_{13}f}+X_{S1}= \\ &-(f+Z_{S2})\frac{a_{21}x_2+a_{22}y_2-a_{23}f}{c_{21}x_2+c_{22}y_2-c_{23}f}+X_{S2} \\ &-(f+Z_{S1})\frac{b_{11}x_1+b_{12}y_1-b_{13}f}{c_{11}x_1+c_{12}y_1-c_{13}f}+Y_{S1}= \\ &-(f+Z_{S2})\frac{b_{21}x_2+b_{22}y_2-b_{23}f}{c_{21}x_2+c_{22}y_2-c_{23}f}+Y_{S2} \end{aligned}\right\} \quad (5)$$

Where, f : Focal length

(X_{Si}, Y_{Si}, Z_{Si}): the coordinate of projective center S_i

$\begin{bmatrix} a_{i1} & a_{i2} & a_{i3} \\ b_{i1} & b_{i2} & b_{i3} \\ c_{i1} & c_{i2} & c_{i3} \end{bmatrix}$: the rotation matrix of image p_i

(x_i, y_i): the coordinate of image point a_i（i = 1,2）.

To calculate the coordinate difference between correspondingly projective points, Eqs.5 is transform to Eqs.6.

$$\left.\begin{aligned} &\Delta X=-(f+Z_{S1})\frac{a_{11}x_1+a_{12}y_1-a_{13}f}{c_{11}x_1+c_{12}y_1-c_{13}f}+X_{S1}+ \\ &(f+Z_{S2})\frac{a_{21}x_2+a_{22}y_2-a_{23}f}{c_{21}x_2+c_{22}y_2-c_{23}f}-X_{S2} \\ &\Delta Y=-(f+Z_{S1})\frac{b_{11}x_1+b_{12}y_1-b_{13}f}{c_{11}x_1+c_{12}y_1-c_{13}f}+Y_{S1}+ \\ &(f+Z_{S2})\frac{b_{21}x_2+b_{22}y_2-b_{23}f}{c_{21}x_2+c_{22}y_2-c_{23}f}-Y_{S2} \end{aligned}\right\} \quad (6)$$

According to the theory of optic projection, the corresponding rays of each image can intersect each other on the public projective plane via adjusting the EOPs of each image. Namely, the least square adjustment system deduced on basis of Eqs.6 is employed to calculate the EOPs following the principle that all of coordinate difference between correspondingly projective points is least square.

Eqs. 7 is the formula describing the displacement of projecting points in the easel plane caused by small angle.

$$\begin{aligned} dX &= db_x+\frac{X}{H}db_z+(H+\frac{X^2}{H})d\varphi+\frac{XY}{H}d\omega-Yd\kappa \\ dY &= db_y+\frac{Y}{H}db_z+\frac{XY}{H}d\varphi+(H+\frac{Y^2}{H})d\omega+Xd\kappa \end{aligned} \quad (7)$$

Then, the observation equation is：

$$\begin{aligned} v_{\Delta X} &= dX_1-dX_2-(X_1^0-X_2^0) \\ v_{\Delta Y} &= dY_1-dY_2-(Y_1^0-Y_2^0) \end{aligned} \quad (8)$$

where：

$$\begin{aligned} dX_i &= db_{xi}+\frac{X_i^0}{H}db_{zi}+(H+\frac{X_i^{0\,2}}{H})d\varphi_i+\frac{X_i^0Y_i^0}{H}d\omega_i-Y_i^0d\kappa_i \\ dY_i &= db_{yi}+\frac{Y_i^0}{H}db_{zi}+\frac{X_i^0Y_i^0}{H}d\varphi_i+(H+\frac{Y_i^{0\,2}}{H})d\omega_i+X_i^0d\kappa_i \\ X_i^0 &= -(f+Z_{Si})\frac{a_{i1}x_i+a_{i2}y_i-a_{i3}f}{c_{i1}x_i+c_{i2}y_i-c_{i3}f}+X_{Si} \\ Y_i^0 &= -(f+Z_{Si})\frac{b_{i1}x_i+b_{i2}y_i-b_{i3}f}{c_{i1}x_i+c_{i2}y_i-c_{i3}f}+Y_{Si} \end{aligned}$$

Finally, the relatively spatial relationship of the image sequence is determined by the least square adjustment system deduced above and a method similar to ortho-image generation is employed to generate the whole facade texture, as Fig. 7.

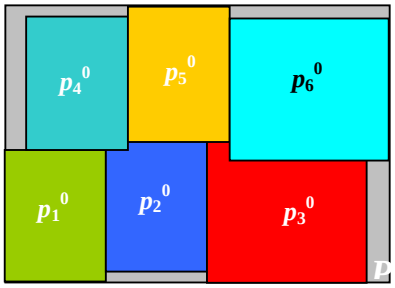

Fig.7 The generation of mosaic image

5. REFINING OF MOSAIC RESULT

As presented above, the mosaic result of vehicle-based imagery is optimized employed the strip method. However, the observation values in the least square adjustment system deduced above are the coordinates of corresponding points. Therefore the mosaic results in those areas having few corresponding points matched are not perfect, as Fig 8.a and Fig

11.a illustrated.

In this section, two refining strategy are presented. One is refining the mosaic region where corresponding points are difficult to be matched but there are plenty of horizontal lines. The constraint of correspondingly horizontal lines is introduced to implement this process. The other is refining the mosaic region by densifying the corresponding points according to the relatively spatial relationship of the image sequence.

5.1 The constraint of correspondingly horizontal lines

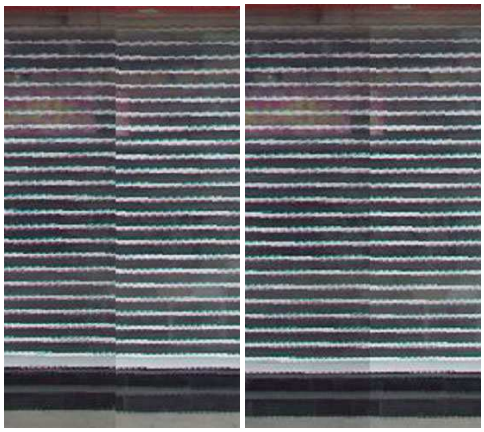

a. Before refining **b.** After refining

Fig. 8 The refined result with constraint of correspondingly horizontal lines

As Fig. 9 illustrated, although few corresponding points in this area, there are plenty of horizontal lines. Therefore, the question is how to match corresponding lines. Firstly, those lines are projected into the mosaic image. Included range of corresponding line is then determined for every line in the left image. As Fig. 10 illustrated, so-called included range is a horizontal strip which center is line L_0 and width is twice as dY. dY is the Y component of the projective difference of the corresponding points near line L_0. Since lines in Fig. 10 are horizontal, the center A_0 of line L_0 is employed to determine corresponding lines. Therefore, those lines in the right image are corresponding lines if their center points (A_1 and A_2) are within the included range of L_0. As we can see, the projective difference ΔY_1 and ΔY_2 between line L_0 and L_1, L_2 are equal to the Y coordinate difference between center A_0 and A_1, A_2. Therefore, the refining strategy for the mosaic result is to make ΔY be the least square by the least square adjustment. The mosaic result is illustrated as Fig. 8b after refining process. As we can see, it's much better after imposing the constraint of correspondingly horizontal lines.

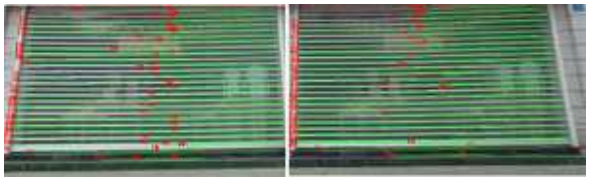

Fig.9 The determination of corresponding lines

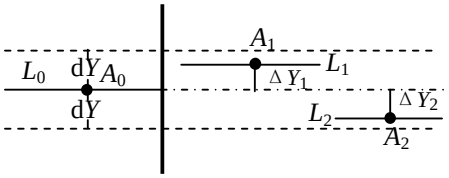

Fig.10 The included range of corresponding lines

5.2 Densifying the corresponding points

As Fig.11a illustrated, the reason for stagger along the mosaic edge is lacking corresponding points in this area. Therefore the best way to refine the result is to densify the corresponding points. As presented in section 3, the projective difference between corresponding points in the mosaic image becomes very small after the least square adjustment. As a result, it is possible to densify the corresponding points in the mosaic image.

a. Before refining **b.** After refining

Fig.11 The refining result by densifying corresponding points

The region need to be densify should be determined firstly. For this purpose, a grid is overlaid on the image. The size of grid is depends on the size of image. The image size in Fig. 11 is 1000 pixels×1500 pixels and a 20×20 grid is overlaid. Therefore, the grid cell size is 50 pixels×75 pixels. Those grid cells overlaid in the region of sky are thrown off according to roof

boundary tracked (Blue curve in the image) because it is useless to densify corresponding points in the region of sky. Those grid cells with few corresponding points included should be the regions to densify corresponding points. Then, corresponding points are matched in these regions. The projective difference, between the existing corresponding points near or in these regions, can be employed to forecast the position of corresponding points. More corresponding point are matched according to the position forecasted, as Fig. 11b illustrated. Finally, those corresponding points are added to the least square adjustment system. The mosaic result refined by the strategy densifying the corresponding points is illustrated as Fig. 11b. From the result we can see that the stagger existing in Fig. 11a is eliminated in b.

6. EXPERIMENTAL RESULTS

Experiments were implemented on side-shooting image sequences (Fig.12) taken by digital camera KODAK PROFESSIONAL DCS Pro SLR/n along the pedestrian street. The distance between photographic center and building is about 10m. The image size is 3000 pixels×4500 pixels. To fix the interior parameter during the process of taking photos, the focal length is set to infinitude and the function of automatic focalization is turned off. Actually, it's not necessary to process the imagery with such large image size, therefore, the raw images were compressed and image size is reduced to 1500 pixels×1000 pixels.

Fig.12 Side-shooting image sequence

Fig.13 A segment of street facade

Both of image sequence subsection and strip method are based on the rectification of raw image, therefore, an algorithm based on vanishing point geometry and geometric constrains of parallel object lines presented in Section 2 is used to automatic rectify the raw image. The average time consuming for the rectification of a single image is 30 seconds. As a 82m long building facade as be concerned, the number of raw images is 36 and total time of rectification becomes 18 minutes.

Experiment was implemented on automatic image sequence subsection using the method presented in Section 3. As shown in Fig.13 a 146 meters long segment of street facade consists of two cross-roads and four connected buildings. There are 58 images taken to cover this segment. The histograms of projective difference of corresponding points (Fig.14) were generated to indicate the position of large range variance from those images. In Fig.14, the positions of peak values exactly indicate the positions in the raw images (Fig.15) of two cross-roads and the building (highlighted in a red rectangle in Fig.13) which has large range difference with others.

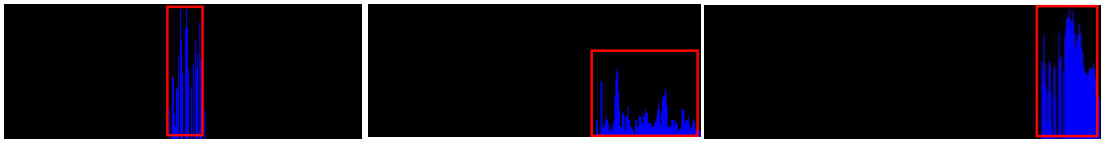

a Cross-road *A* *b* Connected building *c* Cross-road *B*

Fig.14 The histograms of projective difference of corresponding points

a Cross-road *A* *b* Connected building *c* Cross-road *B*

Fig.15 Large range variance in raw images

According to the position detected, two image segments were subsected from 58 images and automatically corresponded to the buildings of interest because images were taken along the

street in sequence.

After the subsection of image sequence, every building has a corresponding image segment to recover facade texture. As presented in Section 4, image mosaic is required to generate the whole facade texture. For comparison, facade texture is mosaicked from close-ranged digital camera images respectively by the existing image mosaic software and the strip method presented in Section 4. The results of image mosaic software Supresoft ImageSuite and Cannon Photostich are shown in Fig.16. Obviously, the existing software tools of image mosaic are not applicable for processing images with large obliquity of the posture of digital camera. As Fig. 17 illustrated, the mosaic result was acquired using the strip method and refined by the two strategies presented in Section 5. Obviously it is satisfying and realizing the seamless mosaic. As the 82m long building facade as be concerned, there are 216 unknown parameters in the adjustment system of strip method and the time consuming is only 10 seconds. The whole process is fully automatic and fast.

a. ImageSuite ***b*** **.**PhotoStitch

Fig.16 Mosaic results by existing software

7. CONCLUSIONS

This paper presented an automatic mosaicking algorithm that can generate the entire facade texture of large buildings from the close-range color images with the considerable geometric distortion due to the large oblique angle. The experimental results indicate that the proposed automatic mosaicking algorithm is effective and reliable for building facade texture mapping. Moreover, the performed tests have revealed several advantages.

- Because the acquisition way of image sequence is vehicle-based and moreover the recovery of building facade texture which is always low efficiency to existing methods realizes automation in our method, the whole process from data acquisition to the generation of building facade texture is implemented in a rapid and high efficient way.
- Terrestrial close-ranged images have high resolution and moreover are taken along street, therefore a walk-through 3D scene closing to the reality can be reconstruct.

The approach presented in this paper is applicable for streets with high density of buildings. Future work will concentrate on the 3D model reconstruction for more complex facade and improvement of availability.

REFERENCES

References from Journals:

Caprile, B. and V. Torre, 1990. Using vanishing points for camera calibration, *International Journal of Computer Vision*, 4(2): 127–140.

References from Other Literature:

Antone, M.E.; Teller, S. **"**Automatic recovery of relative camera rotations for urban scenes. " Proc. IEEE Conf. on Computer Vision and Pattern Recognition, Hilton Head Island, 2000, p.282-9.

Frueh, C., R. Sammon, and A. Zakhor, 2004. Automated texture mapping of 3D city models with oblique aerial imagery, *Proceedings of the 2nd International Symposium on 3D Data*

Fig.17 Whole facade texture

Processing, Visualization and Transmission (3DPVT 2004). 6 - 9 September, Thessaloniki, Greece, pp. 396-403.

Früh, C. and A. Zakhor, 2001. Fast 3D model generation in urban environments, Proceedings of IEEE Conference on Multisensor Fusion and Integration for Intelligent Systems, pp. 165 - 170.

Stamos, I.; Allen, P.E. "3-D model construction using range and image data." Proceedings IEEE Conf. on Computer Vision and Pattern Recognition, Hilton Head Island, 2000, p.531-6.

Takase, Y., N. Sho, A. Sone and K. Shimiya, 2003. Automatic generation of 3D city models and related applications, *International Archives of the Photogrammetry, Remote Sensing and Spatial Information Sciences*, 24-28 February, Tarasp, Switzerland, 34(5/W10)

Thrun, S.; Burgard, W.; Fox, D.: "A real-time algorithm for mobile robot mapping with applications to multi-robot and 3D mapping"**,** Proc. of International Conference on Robotics and Automation, San Francisco, 2000, p..321-8, vol. 1. 4

Acknowledgements

This research was supported by the National High Technology Research and Development Program of China (863 Program) with the serial number 2006AA12Z220.